nature geoscience

ARTICLES

PUBLISHED ONLINE: 30 JANUARY 2011 | DOI: 10.1038/NGEO1065

Complex layered deformation within the Aegean crust and mantle revealed by seismic anisotropy

Brigitte Endrun[1]*, Sergei Lebedev[2], Thomas Meier[3], Céline Tirel[2] and Wolfgang Friederich[4]

Continental lithosphere can undergo pervasive internal deformation, often distributed over broad zones near plate boundaries. However, because of the paucity of observational constraints on three-dimensional movement at depth, patterns of flow within the lithosphere remain uncertain. Endmember models for lithospheric flow invoke deformation localized on faults or deep shear zones or, alternatively, diffuse, viscous-fluid-like flow. Here we determine seismic Rayleigh-wave anisotropy in the crust and mantle of the Aegean region, an archetypal example of continental deformation. Our data reveal a complex, depth-dependent flow pattern within the extending lithosphere. Beneath the northern Aegean Sea, fast shear wave propagation is in a North–South direction within the mantle lithosphere, parallel to the extensional component of the current strain rate field. In the south-central Aegean, where deformation is weak at present, anisotropic fabric in the lower crust runs parallel to the direction of palaeo-extension in the Miocene. The close match of orientations of regional-scale anisotropic fabric and the directions of extension during the last significant episodes of deformation implies that at least a large part of the extension in the Aegean has been taken up by distributed viscous flow in the lower crust and lithospheric mantle.

In the course of the slow convergence of the African and Eurasian plates in the Eastern Mediterranean, oceanic basins have been subducted north-northeastwards and continental blocks have been accreted to what is now the Aegean[1–4]. The region-scale south-southwestward extension in the Aegean has been associated with the retreat of the Hellenic Trench[4–7] and is estimated to be by as much as 580 km since the Mid-Eocene[1].

The extension was accompanied by exhumation of extensional domes (metamorphic core complexes, MCCs) in the Rhodope, the Cyclades, and elsewhere[1,4,8]. The stretching lineations now observed in the exhumed rocks are indicators of the Oligocene–Miocene extension directions. In the central Aegean, the orientation of the lineations is roughly northeast–southwest (NE–SW) across most of the Cyclades[9], with the exception of the islands southeast of the Mid-Cycladic lineament that have undergone counter-clockwise rotation and now show north–south (N–S) lineations (Figs 1a, 2b). According to palaeomagnetic data, the lineations across the Cyclades are likely to have been uniformly NE–SW before the Mid to Late Miocene rotations[9,10].

After about 5 Myr ago the North Anatolian Fault (NAF) propagated into the northern Aegean as the North Aegean Trough (NAT), modifying the deformation regime of the region and accommodating a counter-clockwise rotation of the Aegean and Anatolian lithospheres[11]. The extension directions in the northern Aegean Sea changed from probable NE–SW in the Miocene to N–S at present[10,12–14]. In the central Aegean, the Cyclades have undergone little recent deformation, behaving as a nearly rigid block[10,13–15].

Global Positioning System (GPS) measurements[13–15] show that the current surface velocity field in the Aegean is dominated by the west-southwestward motion of the entire Aegean domain south of the NAT, probably driven by the retreat of the subduction zone (Fig. 1). In addition to this translational motion, the northern Aegean Sea (between the NAT to the North and the Cyclades to the South) is undergoing N–S extension[13,14]. The style of the deformation that accommodates the extension is disputed. In the brittle upper crust, much of the deformation is taken up by slip on a system of NE–SW trending strike-slip faults, rotating counter-clockwise[12,16,17]. Relative to Eurasia, the GPS vectors point west-southwest in northwestern Anatolia and southwest in eastern Greece, showing that the deforming northern Aegean Sea undergoes a substantial counter-clockwise rotation. Such rotation is consistent with strike-slip faulting accommodating much of the N–S extension. In addition, a part of the extension is accommodated by stretching, evidenced by Plio-Quaternary sedimentary basins and normal-fault earthquakes[12,13,18]. Intraplate seismicity at numerous, broadly distributed minor faults has been interpreted as evidence for a substantial component of distributed deformation[15,19], but the proportions of the extension taken up by the localized and diffuse deformation have been a matter of debate[11–13,15,16,19–21]. The deep lithosphere, comprising the lower crust and lithospheric mantle, is likely to play a key role in the dynamics of extension[22–24]. Deep lithospheric deformation, however, has been difficult to constrain directly.

Seismic anisotropy

Measurements of seismic anisotropy offer observational constraints on the past and present deformation in the deep lithosphere and mantle below. Finite strain within the crust and mantle results in the lattice preferred orientation (LPO) of anisotropic major minerals, including amphibole and olivine in the lower crust and upper mantle, respectively[25–27]. The LPO gives rise to the directional dependence of seismic wavespeeds, or seismic anisotropy. If a sufficient amount of finite strain accumulates with the same deformation pattern, directions of fastest seismic-wave propagation will match the directions of maximum extension[25,28].

Recent observations of strong splitting of SKS waves in the Aegean (1.0–1.5 s across much of the region, locally up to 2.4 s) are evidence for substantial seismic anisotropy at depth[29,30]. Because

[1]Institute of Earth and Environmental Sciences, University of Potsdam, Karl-Liebknecht-Straße 24, 14476 Potsdam, Germany, [2]Dublin Institute for Advanced Studies, Geophysics Section, 5 Merrion Square, Dublin 2, Ireland, [3]Institute of Geosciences, Christian-Albrechts University of Kiel, Otto-Hahn-Platz 1, 24118 Kiel, Germany, [4]Institute of Geology, Mineralogy and Geophysics, Ruhr-University Bochum, 44780 Bochum, Germany. *e-mail: brigitte.endrun@geo.uni-potsdam.de.

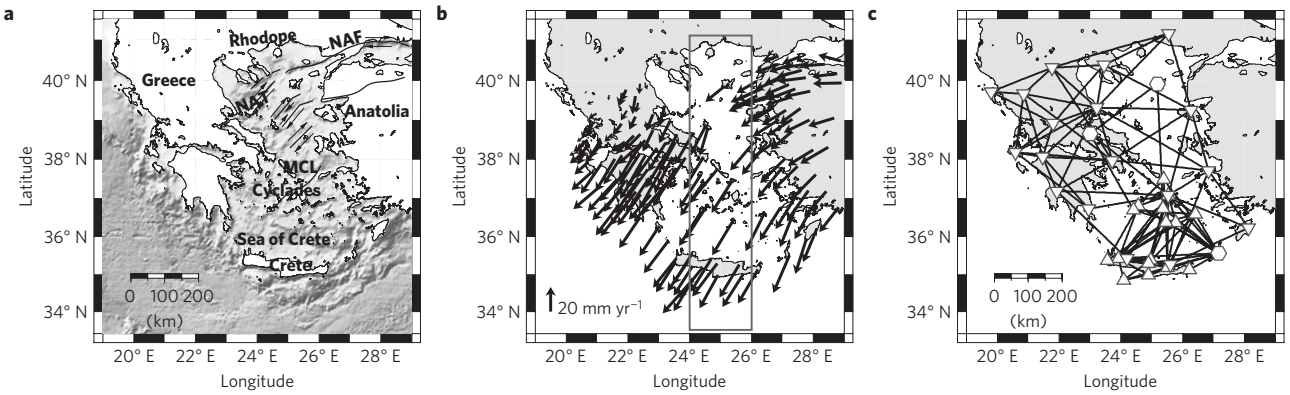

Figure 1 | The study area and path coverage. a, Tectonic setting of the Aegean region, showing major faults[12,16–19], the Mid-Cycladic Lineament (MCL; refs 1,10) and the North Aegean Trough (NAT). **b**, Selected, representative GPS velocities in a Eurasia reference frame[15]. The rectangle shows the area of the cross-section in Fig. 4. **c**, Interstation path coverage used for Rayleigh-wave tomography. Different symbols refer to different station types (see ref. 40 for details on instrumentation).

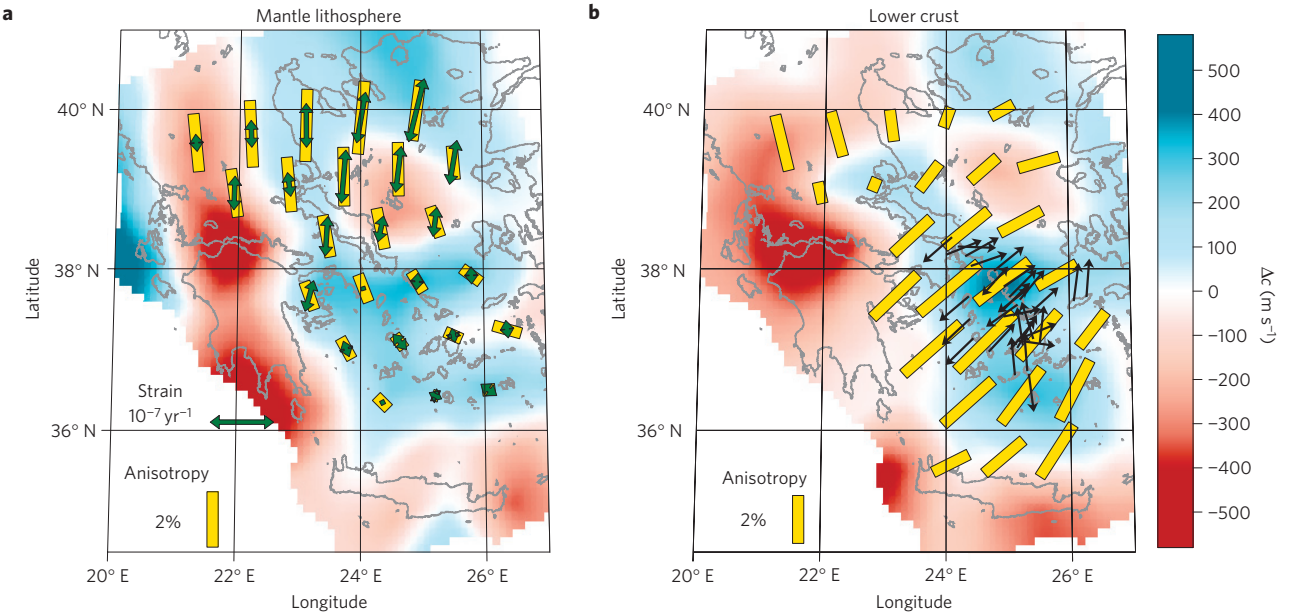

Figure 2 | Anisotropic phase-velocity maps. Rayleigh waves at the periods sampling primarily the lithospheric mantle (30 s, average reference velocity 3.77 km s^{-1}, **a**) and the lower crust (15 s, average reference velocity 3.24 km s^{-1}, **b**). Yellow bars indicate fast axes of anisotropy. Green arrows in **a** show the extensional component of the current strain field from the Global Strain Rate Map project[41]. Black arrows in **b** show Miocene stretching lineations[9] (simplified) indicative of directions of palaeo-extension.

SKS splitting measurements are weakly sensitive to the distribution of anisotropy with depth, it is difficult to relate them directly to the vertical distribution of strain and to lithospheric dynamics. Surface waves are the type of data that can provide the necessary vertical resolution[31–37]. Analysis of surface-wave data has been used in recent studies to map distributions of azimuthal seismic anisotropy in increasing detail, both laterally and vertically[34–36,38,39].

In this study we use a large Rayleigh-wave data set measured in the Aegean[40] and constrain the layering of seismic anisotropy beneath the region. Phase velocities of the fundamental mode were measured, with an elaborate recent implementation of the two-station method[2], along 98 paths between 37 stations from different temporary and permanent digital broadband networks (Fig. 1, Supplementary Figs S1 and S2). A comparison of dispersion curves from different parts of the Aegean shows large structural variations across the region (Supplementary Fig. S3).

Combining all our measurements, we perform tomographic inversions and compute azimuthally anisotropic phase-velocity maps. The isotropic component of the tomographic solutions reflects lateral variations in isotropic shear speeds and in the crustal thickness. The largest variability is observed at the 25-s period and is due to variations in the depth of the crust–mantle transition. The low-velocity wedge above the slab is seen as a prominent anomaly along the forearc (Fig. 2).

Interestingly, the deforming lithosphere of the northern Aegean Sea displays lower seismic velocities than the non-deforming central Aegean lithosphere (Fig. 2). This seismic-velocity contrast may indicate a viscosity contrast that governs the distribution of deformation across the sea. Higher temperature or, alternatively, higher water content would decrease both seismic velocity and the strength of the lithosphere. Modification of the lithosphere due to magmatism may also have played a role.

The anisotropic component of the tomographic solutions reflects the presence of anisotropic fabric in the crustal and mantle rocks. The amplitude of phase-velocity anisotropy we observe reaches 3.5–3.75% of the isotropic average at shorter,

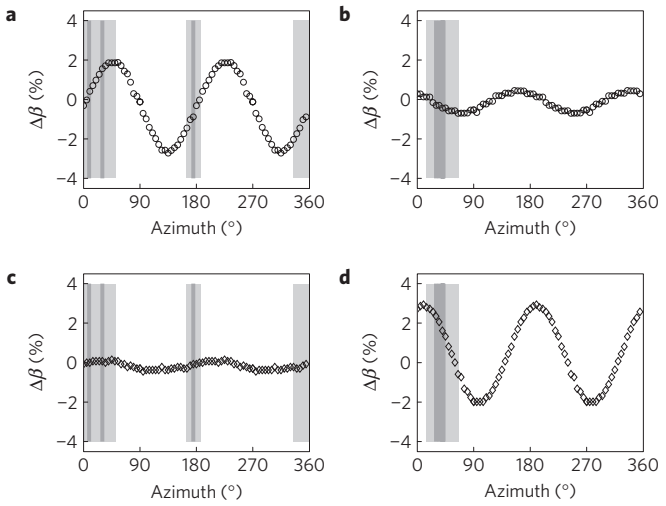

Figure 3 | S-wave velocity variations with azimuth. The anisotropic patterns are for the south-central Aegean mid-lower crust (**a**) and lithospheric mantle (**c**) and the northern Aegean mid-lower crust (**b**) and lithospheric mantle (**d**). Fast splitting directions from SKS measurements in the same areas[29,30] are indicated by grey bars (dark grey–average direction, light grey–standard deviations).

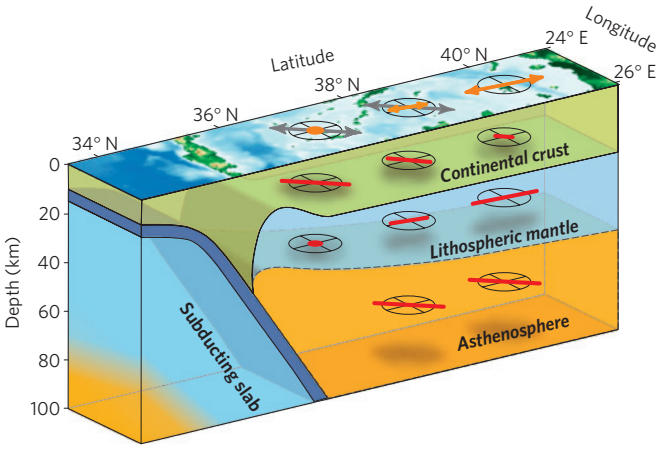

Figure 4 | Azimuthal anisotropy in the lower crust and upper mantle of the Aegean Sea. This synthesis is consistent with both surface-wave (this study) and SKS-splitting[29,30] data. Red bars show the fast S-wave propagation directions. Orange arrows on the map on top of the cross-section show directions of the extension active today[41]; grey arrows show the Miocene extension directions[9,10].

crustal periods and decreases at longer periods. We verify the robustness of the models with a series of resolution tests (Supplementary Figs S4–S9). In Fig. 2 we plot the robust, well-resolved anisotropic anomalies.

Deformation in the northern Aegean Sea

The directions of fast propagation of Rayleigh waves at a period of 30 s, sampling primarily the lithospheric mantle in the 30–70 km depth range (Supplementary Fig. S10), show a remarkable match with the directions of the extensional component of the current strain field[13–15,21,41], active since about 5 Myr ago[11,12]. Seismic anisotropy in the mantle lithosphere can be explained by the LPO of olivine, developed in response to finite strain[25,28]. Strain rates on the order of 10^{-7} yr^{-1}, as found in the northern Aegean[15,16,21,41], would have produced, if consistently active for 5 Myr, finite strain of 0.5, probably sufficient for the development of the LPO and detectable anisotropy[25,28] (Supplementary Discussion). Our observations are thus consistent with the occurrence of diffuse viscous flow in the mantle lithosphere that accommodates, at least in part, the N–S extension observed at the surface in the northern Aegean Sea (between the NAT and the Cyclades).

Anisotropy at 12–18 s periods, sampling the mid-lower crust, shows an average amplitude of around 1.8% in the northern Aegean. The fast-propagation directions are nearly parallel to the strike-slip faults in the brittle upper crust above (Fig. 1a).

Our results show that the deformation of the northern Aegean Sea lithosphere is coherent in the sense that from the upper crust down to the lithospheric mantle it undergoes the same region-scale, North–South extension. The style of this deformation, however, is different in the brittle upper crust (slip on fault systems) and in the lithospheric mantle (viscous flow), with the ductile mid-lower crust accommodating the transition between the two[22].

Such layering of deformation of different types (brittle in the upper crust, viscous in the lower crust and lithospheric mantle) has been inferred previously for major strike-slip fault systems, including the San Andreas Fault[22] and the Marlborough Fault[42], where the mantle shows flow within relatively broad zones around the faults, in a direction parallel to them. The deformation regime of the northern Aegean Sea is different. The pattern of depth-dependent deformation revealed by seismic anisotropy between the NAT and the Cyclades presents a spectacular demonstration of the viscous behaviour of the mantle lithosphere, which is seen flowing straight in the direction of extension.

The Cyclades

In the south-central Aegean, currently a nearly non-deforming block[13,14,21], strong azimuthal anisotropy of up to 3.5% is found in the lower crust (12–18 s period; Fig. 2b). The approximately NE fast-propagation directions closely match the directions of palaeo-extension in the Miocene, known from the stretching lineations in the lower crustal rocks exhumed in MCCs (refs 9, 20). The exhumation of MCCs throughout the area during that time must have been accompanied—according to tectonic and geodynamic models[9,43]—by pervasive ductile flow in the lower crust. The associated large strains would have produced fabric with a large degree of alignment of lower-crustal anisotropic minerals[44]. With recent strain rates in the south-central Aegean being very low[10], the crustal LPO could not have been overprinted since its formation in the Miocene. The observed anisotropy thus indicates fossil fabric, a record of the region-scale viscous flow in the lower crust that accompanied the extension and MCC exhumation before 5 Myr ago[1,9,11,12].

Seismic anisotropy in the central Aegean mantle lithosphere (25–30 s periods) is small, matching the lack of recent deformation. We suggest that any pre-existing fabric at 40–60 km may have been weakened, possibly owing to the recent thinning of the lithosphere to about 50 km (ref. 40) and accompanying asthenospheric upwelling or to the interaction with subduction-related fluids (Supplementary Discussion).

Layering of anisotropy and deformation

To verify that the distributions of phase-velocity anisotropy (Fig. 2) reflect anisotropy in the lower crust and uppermost mantle depth ranges, we also invert them for azimuthally anisotropic Vs profiles that average across the northern and the south–central Aegean (Supplementary Methods, Fig. S11). The resulting patterns for both the mid-lower-crust and lithospheric-mantle depth ranges are consistent with and confirm our interpretation (Fig. 3).

Fast-propagation azimuths inferred from SKS splitting[29,30] (Fig. 3) show no correlation with fast-propagation directions that we find in the mantle lithosphere (Fig. 3; Supplementary Discussion, Figs S13, S14). The splitting thus cannot be attributed to

LPO in the mantle lithosphere, as has been suggested previously[16]. In the Northern Aegean, SKS-inferred fast-propagation directions (38° azimuth, averaged over five stations) are nearly parallel to the crustal fast-propagation directions that we have determined. The observed splitting times of 1.5 s on average, however, are too large to be caused by crustal anisotropy only (Supplementary Discussion). We conclude that SKS splitting is mainly due to seismic anisotropy at depths greater than 50–60 km, probably in the asthenosphere, although we cannot rule out a deeper origin of the signal (for example, the mantle transition zone). Most probably, SKS splitting reflects strain in the asthenosphere and indicates asthenospheric flow associated with the southwestward retreat of the subduction zone.

We summarize the 3D distribution of azimuthal anisotropy in Fig. 4. The crustal thickness is taken from published seismic and gravity studies[12,40], the lithospheric thickness—from surface-wave analysis[40], the position of the slab—from seismicity, receiver functions and body-wave tomography[45–49]. In the south-central Aegean (the Cyclades), the probably frozen-in fabric in the lower crust trends parallel to the Miocene extension direction. This fabric is a record of pervasive lower-crustal flow that accompanied the extension and the formation of the MCCs (refs 9,10,12). In the northern Aegean, the fabric in the mantle lithosphere trends parallel to the extensional component of the current deformation field, indicating that the extension is taken up, at least in part, by distributed flow in the mantle lithosphere. The northern Aegean mid-lower crust exhibits modest anisotropy with a NE–SW orientation; this layer seems to accommodate a transition between the strike-slip motion on NE–SW trending faults in the brittle upper crust and the N–S viscous flow in the mantle lithosphere. Previously reported shear wave splitting probably originates in the asthenosphere and indicates NE–SW flow there.

The close match of the directions of extension during the last major deformation episodes (present or past) and the regional-scale fabric in the crustal and mantle rocks demonstrates that at least a large part of the extension in the Aegean has been taken up by distributed viscous flow in the lower crust and lithospheric mantle. Depth-dependent azimuthal anisotropy indicates the vertical distribution of finite strain and reveals a complex, three-dimensional pattern of deformation within the lithosphere and asthenosphere, driven by the subduction-zone retreat.

Methods

Anisotropic Rayleigh wave tomography was performed including isotropic and both 2ψ (180°-periodic) and 4ψ (90°-periodic) anisotropic terms (Supplementary Equation 1). Phase velocities at different periods in the 10–30 s range are inverted on a triangular grid with a 75 km knot spacing[50]. The grid spacing of 75 km was determined as optimal from numerous resolution tests. Smoothing is applied independently to the isotropic, 2ψ, and 4ψ inversion parameters. The optimal smoothing parameters were determined by resolution tests. For the isotropic part of the model, the recovery of mixed chequerboard/spike patterns was investigated (Supplementary Fig. S4). The 2ψ (4ψ) smoothing factors were determined using the condition that little spurious anisotropy should be introduced when inverting purely isotropic (isotropic and 2ψ) synthetic data (Supplementary Fig. S5). The smoothing has enabled us to determine larger-scale isotropic and 2ψ-term anisotropy patterns that are robust and, in particular, insensitive to whether variations in 4ψ-term anisotropy are included in tomographic solutions (Supplementary Figs S6–S8).

During the tomographic inversion, each dispersion curve was weighted by the size of its 99% confidence limits to reduce the influence of more uncertain data. When projecting the measurements along the raypaths, we used a sensitivity area of finite width[50]. Tomographic inversions were performed independently for different periods.

Received 10 August 2010; accepted 16 December 2010; published online 30 January 2011; corrected online 3 February 2011

References

1. Brun, J-P. & Faccenna, C. Exhumation of high-pressure rocks driven by slab rollback. *Earth Planet. Sci. Lett* **272,** 1–7 (2008).
2. Meier, T., Dietrich, K., Stöckhert, B. & Harjes, H-P. One-dimensional models of shear wave velocity for the eastern Mediterranean obtained from the inversion of Rayleigh wave phase velocities and tectonic implications. *Geophys. J. Int.* **156,** 45–58 (2004).
3. Van Hinsbergen, D. J. J., Hafkenscheid, E., Spakman, W., Meulenkamp, J. E. & Wortel, R. Nappe stacking resulting from subduction of oceanic and continental lithosphere below Greece. *Geology* **33,** 325–328 (2005).
4. Brun, J-P. & Sokoutis, D. 45 m.y. of Aegean crust and mantle flow driven by trench retreat. *Geology* **38,** 815–818 (2010).
5. McKenzie, D. Active tectonics of the Mediterranean region. *Geophys. J. R. Astron. Soc.* **30,** 109–185 (1972).
6. Le Pichon, X. & Angelier, J. The Aegean Sea. *Phil. Trans. R. Soc. Lond. A* **300,** 357–372 (1981).
7. Jolivet, L. & Faccenna, C. Mediterranean extension and the Africa–Eurasia collision. *Tectonics* **19,** 1095–1106 (2000).
8. Lister, G. S., Banga, G. & Feenstra, A. Metamorphic core complexes of Cordilleran type in the Cyclades, Aegean Sea, Greece. *Geology* **12,** 221–225 (1984).
9. Tirel, C., Gautier, P., van Hinsbergen, D. J. J. & Wortel, M. J. R. in *Collision and Collapse at the Africa–Arabia–Eurasia Subduction Zone* 311 (eds van Hinsbergen, D. J. J., Edwards, M. A. & Govers, R.) 257–292 (Spec. Publ. Geol. Soc. Lond., 2009).
10. Walcott, C. R. & White, S. H. Constraints on the kinematics of post-orogenic extension imposed by stretching lineations in the Aegean region. *Tectonophysics* **298,** 155–175 (1998).
11. Armijo, R., Meyer, B., King, G. C. P., Rigo, A. & Papanastassiou, D. Quaternary evolution of the Corinth Rift and its implications for the Late Cenozoic evolution of the Aegean. *Geophys. J. Int.* **126,** 11–53 (1996).
12. Tirel, C., Gueydan, F., Tiberi, C. & Brun, J-P. Aegean crustal thickness inferred from gravity inversion. Geodynamical implications. *Earth Planet. Sci. Lett.* **228,** 267–280 (2004).
13. McClusky, A. *et al.* Global Positioning System constraints on plate kinematics and dynamics in the eastern Mediterranean and Caucasus. *J. Geophys. Res.* **105,** 5695–5719 (2000).
14. Reilinger, R., McClusky, S., Paradissis, D., Ergintav, S. & Philippe Vernant, P. Geodetic constraints on the tectonic evolution of the Aegean region and strain accumulation along the Hellenic subduction zone. *Tectonophysics* **488,** 22–30 (2010).
15. Floyd, M. A. *et al.* A new velocity field for Greece: Implications for the kinematics and dynamics of the Aegean. *J. Geophys. Res.* **115,** B10403 (2010).
16. Kreemer, C., Chamot-Rooke, N. & Le Pichon, X. Constraints on the evolution and vertical coherency of deformation in the Northern Aegean from a comparison of geodetic, geologic and seismologic data. *Earth Planet. Sci. Lett.* **225,** 329–346 (2004).
17. Taymaz, T., Jackson, J. & McKenzie, D. Active tectonics of the north and central Aegean Sea. *Geophys. J. Int.* **106,** 433–490 (1991).
18. Mascle, J. & Martin, L. Shallow structure and recent evolution of the Aegean Sea: A synthesis based on continuous reflection profiles. *Mar. Geol.* **94,** 271–299 (1990).
19. Papazachos, C. B. & Kiratzi, A. A detailed study of the active crustal deformation in the Aegean and surrounding area. *Tectonophysics* **253,** 129–153 (1996).
20. Jolivet, L., Faccenna, C. & Piromallo, C. From mantle to crust: Stretching the Mediterranean. *Earth Planet. Sci. Lett.* **285,** 198–209 (2009).
21. LePichon, X. & Kreemer, C. The Miocene-to-present kinematic evolution of the Eastern Mediterranean and Middle East and its implications for dynamics. *Annu. Rev. Earth Planet. Sci.* **38,** 323–351 (2010).
22. Bourne, S. J., England, P. C. & Parsons, B. The motion of crustal blocks driven by flow of the lower lithosphere and implications for slip rates of continental strike-slip faults. *Nature* **391,** 655–659 (1998).
23. Molnar, P. & Tapponier, P. Cenozoic tectonics of Asia: Effects of a continental collision. *Science* **189,** 419–426 (1975).
24. Molnar, P. Continental tectonics in the aftermath of plate tectonics. *Nature* **335,** 131–137 (1988).
25. Ribe, N. M. On the relation between seismic anisotropy and finite strain. *J. Geophys. Res.* **97,** 8737–8747 (1992).
26. Tommasi, A., Mainprice, D., Canova, G. & Chastel, Y. Viscoplastic self-consistent and equilibrium-based modeling of olivine lattice preferred orientations: Implications for the upper mantle seismic anisotropy. *J. Geophy. Res.* **105,** 7893–7908 (2000).
27. Tatham, D. J., Lloyd, G. E., Butler, R. W. H. & Casey, M. Amphibole and lower crustal seismic properties. *Earth Planet. Sci. Lett.* **267,** 118–128 (2008).
28. Becker, T. W., Chevrot, S., Schulte-Pelkum, V. & Blackman, D. K. Statistical properties of seismic anisotropy predicted by upper mantle geodynamic models. *J. Geophys. Res.* **111,** B08309 (2006).
29. Hatzfeld, D. *et al.* Shear wave anisotropy in the upper mantle beneath the Aegean related to internal deformation. *J. Geophys. Res.* **106,** 30737–30753 (2001).
30. Schmid, C., van der Lee, S. & Giardini, D. Delay times and shear wave splitting in the Mediterranean region. *Geophys. J. Int.* **159,** 275–290 (2004).

31. Montagner, J-P. & Nataf, H-C. A simple method for inverting the azimuthal anisotropy of surface waves. *J. Geophys. Res.* **91,** 511–520 (1986).
32. Montagner, J-P. & Tanimoto, T. Global upper mantle tomography of seismic velocities and anisotropies. *J. Geophys. Res.* **96,** 20337–20351 (1991).
33. Shapiro, N. M., Ritzwoller, M. H., Molnar, P. & Levin, V. Thinning and flow of Tibetan crust constrained by seismic anisotropy. *Science* **305,** 233–236 (2004).
34. Pedersen.H. A., Bruneton.M., Maupin.V. & SVEKALAPKO Seismic Tomography Working group. Lithospheric and sublithospheric anisotropy beneath the Baltic shield from surface-wave array analysis. *Earth Planet. Sci. Lett.* **244,** 590–605 (2006).
35. Yang, Y. & Forsyth, D. W. Rayleigh wave phase velocities, small-scale convection, and azimuthal anisotropy beneath southern California. *J. Geophys. Res.* **111,** B07306 (2006).
36. Marone, F. & Romanowicz, B. The depth distribution of azimuthal anisotropy in the continental upper mantle. *Nature* **447,** 198–201 (2007).
37. Moschetti, M. P., Ritzwoller, M. H., Lin, F. & Yang, Y. Seismic evidence for widespread western-US deep-crustal deformation caused by extension. *Nature* **464,** 885–889 (2010).
38. Zhang, X., Paulssen, H., Lebedev, S. & Meier, T. Surface wave tomography of the Gulf of California. *Geophys. Res. Lett.* **34,** L15305 (2007).
39. Deschamps, F., Lebedev, S., Meier, T. & Trampert, J. Stratified seismic anisotropy reveals past and present deformation beneath the East-central United States. *Earth Planet. Sci. Lett.* **274,** 489–498 (2008).
40. Endrun, B., Meier, T., Lebedev, S., Bohnhoff, M., Stavrakakis, G. & Harjes, H-P. S velocity structure and radial anisotropy in the Aegean region from surface wave dispersion. *Geophys. J. Int.* **174,** 593–616 (2008).
41. Kreemer, C., Holt, W. E. & Haines, A. J. An integrated global model of present-day plate motions and plate boundary deformation. *Geophys. J. Int.* **154,** 8–34 (2003).
42. Molnar, P. *et al.* Continuous deformation versus faulting through the continental lithosphere of New Zealand. *Science* **286,** 516–519 (1999).
43. Block, L. & Royden, L. H. Core complex geometries and regional scale flow in the lower crust. *Tectonics* **9,** 557–567 (1990).
44. Mainprice, D. & Nicolas, A. Development of shape and lattice preferred orientations: Application to the seismic anisotropy of the lower crust. *J. Struct. Geol.* **11,** 175–189 (1989).
45. Papazachos, B. C., Karakostas, V. G., Papazachos, C. B. & Scordilis, E. M. The geometry of the Wadati–Benioff zone and the lithospheric kinematics in the Hellenic arc. *Tectonophysics* **319,** 275–300 (2000).
46. Meier, T. *et al.* in *The Geodynamics of the Aegean and Anatolia* 291 (eds Taymaz, T., Yilmaz, Y. & Dilek, Y.) 183–199 (Spec. Publ. Geol. Soc. Lond., 2007).
47. Endrun, B., Ceranna, L., Meier, T., Bohnhoff, M. & Harjes, H-P. Modeling the influence of Moho topography on receiver functions: A case study from the central Hellenic subduction zone. *Geophys. Res. Lett.* **32,** L12311 (2005).
48. Wortel, M. J. R. & Spakman, W. Subduction and slab detachment in the Mediterranean–Carpathian region. *Science* **290,** 1910–1917 (2000).
49. Piromallo, C. & Morelli, A. *P* wave tomography of the mantle under the Alpine–Mediterranean area. *J. Geophys. Res.* **108,** 2065 (2003).
50. Lebedev, S. & van der Hilst, R. D. Global upper-mantle tomography with the automated multimode inversion of surface and *S*-wave forms. *Geophys. J. Int.* **173,** 505–518 (2008).

Acknowledgements

This work was funded by the German Research Foundation within Collaborative Research Centre SFB 526 'Rheology of the Earth' and by Science Foundation Ireland (grant 08/RFP/GE01704). Earthquake data were provided by NOA, Greece (thanks to G. Stavrakakis), and GEOFON, GFZ Potsdam. We thank GIPP, GFZ Potsdam, for supplying seismic acquisition systems for CYCNET. The authors acknowledge D. Hatzfeld for contributing a digital version of his SKS data set, E. Sandvol for providing the results of the Pn tomography by Al-Latzki *et al.* (Supplementary Information), and T. Becker for stimulating discussions.

Author contributions

B.E. performed measurements, computed and analysed seismic models, and wrote the first draft. S.L. and T.M. contributed software and revised the manuscript extensively. T.M. initiated the study. T.M. and W.F. secured primary funding for this work. C.T. contributed tectonics and geodynamics expertise and implemented Fig. 4; all authors contributed ideas and discussed the results and implications.

Additional information

The authors declare no competing financial interests. Supplementary information accompanies this paper on www.nature.com/naturegeoscience. Reprints and permissions information is available online at http://npg.nature.com/reprintsandpermissions. Correspondence and requests for materials should be addressed to B.E.

ERRATUM

Complex layered deformation within the Aegean crust and mantle revealed by seismic anisotropy

Brigitte Endrun, Sergei Lebedev, Thomas Meier, Céline Tirel and Wolfgang Friederich

Nature Geoscience doi:10.1038/ngeo1065 (2011); published online: 30 January 2011; corrected online: 2 February 2011.

In the version of this Article originally published online, the label 'Lower crust' was missing from the top of Fig. 2b. This error has now been corrected in all versions of the text.